Instabilities of High Speed Dislocations

J. Verschueren,[1,*] B. Gurrutxaga-Lerma,[2,3,†] D. S. Balint,[4] A. P. Sutton,[5] and D. Dini[4]
[1]Department of Materials, Imperial College London, London SW7 2AZ, United Kingdom
[2]Trinity College, University of Cambridge, CB2 1TQ Cambridge, United Kingdom
[3]Department of Engineering, University of Cambridge, CB2 1PZ Cambridge, United Kingdom
[4]Department of Mechanical Engineering, Imperial College London, London SW7 2AZ, United Kingdom
[5]Department of Physics, Imperial College London, London SW7 2AZ, United Kingdom

(Received 16 July 2018; published 2 October 2018)

Despite numerous theoretical models and simulation results, a clear physical picture of dislocations traveling at velocities comparable to the speed of sound in the medium remains elusive. Using two complementary atomistic methods to model uniformly moving screw dislocations, lattice dynamics and molecular dynamics, the existence of mechanical instabilities in the system is shown. These instabilities are found at material-dependent velocities far below the speed of sound. We show that these are the onset of an atomistic kinematic generation mechanism, which ultimately results in an avalanche of further dislocations. This homogeneous nucleation mechanism, observed but never fully explained before, is relevant in moderate and high strain rate phenomena including adiabatic shear banding, dynamic fracture, and shock loading. In principle, these mechanical instabilities do not prevent supersonic motion of dislocations.

DOI: 10.1103/PhysRevLett.121.145502

Gliding dislocations dominate the plastic deformation of crystalline materials [1], particularly under high strain rates and shock loading conditions [2,3], and have been studied for almost as long as dislocation theory itself. In these regimes, dislocations are assumed to move en masse without the involvement of kinks [1]. For a Volterra dislocation in a linear elastic continuum, Frank [4] and Eshelby [5,6] found the elastic energy of a uniformly moving dislocation diverged at the transverse speed of sound, which suggested the existence of a *limiting speed* for dislocations. Early experimental studies of dislocation mobility also suggested a saturation of glide speeds as the speed of sound is approached [7–10]. Since then, continuum models of increasing complexity have been proposed to describe dislocation glide [11–18]. The limiting speeds of dislocations found in continuum models have been attributed to inadequate treatments of the dislocation core [18,19] and the inherent limitations of the small strain approximation [20–22].

The insights from continuum elasticity were challenged first by lattice dynamics models of uniformly moving dislocations which explicitly treated dislocation-lattice interactions [23–26]. The greatest success of these early atomistic models was the formulation of selection rules for lattice waves emitted by a dislocation as it travels through a lattice. This radiation is completely absent in continuum models but plays a crucial role in dislocation mobility formulations [27]. None of these atomistic models found an insurmountable limiting velocity for dislocations. This was confirmed in large-scale nonequilibrium molecular dynamics (MD) simulations that have been employed to study dislocation glide in the last 20 years. A consensus has developed that dislocations may achieve supersonic speeds in MD simulations for a variety of metals [28–33]. To our knowledge, there is no experimental evidence to support or refute this view.

Although no hard barriers were found, the early atomistic models did demonstrate the existence of critical dislocation velocities far below the shear wave speed of the crystal, at which the dislocation-lattice system was driven at a resonant frequency. These were found to occur whenever the group and phase velocities of the emitted radiation were equal to the dislocation velocity, prohibiting the energy carried by these lattice waves to escape the dislocation core [23–26]. Although the origins of these resonant velocities were established, their physical implications have not been explored on the grounds that these lattice dynamics models lose physical significance at resonance [24,26,34].

This Letter shows that the dislocation-lattice resonances [23–26] give rise to mechanical instabilities that result in the kinematic generation of screw dislocations.

Using the theory of lattice dynamics we show that the crystal lattice becomes unstable to the generation of new dislocations at these resonances. We then use MD simulations to remove the approximations of lattice dynamics and confirm the kinematic generation of screw dislocations [1,35,36] at speeds close to those predicted by lattice dynamics theory. This enables us to explain previously reported instabilities in atomistic models [29,36,37]. These instabilities may be significant in adiabatic shear banding [38], dynamic fracture, and displacive phase transitions.

To demonstrate the mechanical instability we consider first the interaction between a uniformly moving screw dislocation and vibrations of the crystal lattice, using Kanzaki forces [39]. When imposed on a perfect lattice treated in the harmonic approximation [40] the Kanzaki force distribution gives rise to the expected displacements of the defect it represents. Originally conceived for point defects, the method was extended and shown to be suitable for the treatment of static and uniformly moving screw dislocations [26,41–43]. The displacement field in a lattice due to a Kanzaki force distribution $\mathbf{F}_K$ is [44]

$$\mathbf{u}(\mathbf{r}_i,t)=\sum_j\int_{-\infty}^{\infty}dt'\mathbf{G}(\mathbf{r}_i-\mathbf{r}_j,t-t')\mathbf{F}_K(\mathbf{r}_j,t'),\qquad(1)$$

where $\mathbf{r}_i$ refers to the position of particle i in the lattice and $\mathbf{G}$ is the lattice Green's function matrix [45]. To simplify the notation but without loss of generality, a monatomic lattice has been assumed throughout. The translation invariance of the crystal enables the Fourier transform of the lattice Green's function matrix to be written as [45,46]

$$\tilde{G}_{\alpha\beta}(\mathbf{k},\omega)=\frac{1}{M}\sum_b\frac{\tilde{u}_\alpha(\mathbf{k},b)\tilde{u}^*_\beta(\mathbf{k},b)}{\omega^2(\mathbf{k},b)-\omega^2+2i\Gamma\omega},\qquad(2)$$

where M is the atomic mass, $\omega(\mathbf{k},b)$ is the vibration frequency of the normal mode with wave vector $\mathbf{k}$ and branch index b and $\tilde{\mathbf{u}}$ is its associated normalized polarization vector [45]. Γ is the coefficient of the viscous damping applied to all atoms, introduced to regularize Eq. (2) at the resonant frequencies $\omega=\omega(\mathbf{k},b)$. The normal mode frequencies are determined for the same interatomic potentials as will be used in the MD simulations below.

We consider the case of a uniformly moving screw dislocation with Burgers vector $\mathbf{B}=B\hat{\mathbf{z}}$, propagating with velocity v_d along the x axis passing $x=0$ at $t=0$. The glide plane is defined to lie halfway between 2 lattice planes with normal $\hat{\mathbf{y}}$. A schematic is shown in the inset of Fig. 1. This moving dislocation is generated in a perfect lattice by the Kanzaki forces [26,43,47]

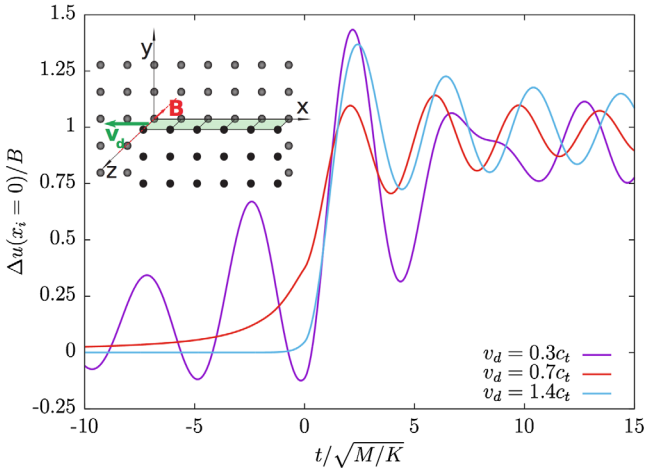

FIG. 1. The relative displacement jump caused by a uniformly moving screw dislocation with velocity v_d in the simple cubic model as computed with lattice dynamics. Note the resonance for $v_d=0.3c_t$.

$$\mathbf{F}_K(\mathbf{r_i})=F_{i\alpha}=\sum_{\beta,j}B\delta_{z\beta}\Psi_{ij}D_{i\alpha j\beta}\times\Theta(v_dt-x_i),\qquad(3)$$

where $\mathbf{D}$ is the matrix of force constants of the lattice, $\Theta(x)$ is the step function, and $\Psi_{ij}=\pm1$ if the particle i is above (below) the glide plane and j below (above), and 0 otherwise. We see from Eq. (3) that this Kanzaki force distribution is nonzero only in a finite region centered on the glide plane equal to the range of the force constants. The lattice symmetry in the z direction is retained and the crystal is treated as a 2D arrangement of infinitely long, rigid atomic rows. The Kanzaki forces, Eq. (3), introduce a relative displacement of atomic rows on either side of the slip plane equal to $\mathbf{B}$. From Eq. (3) we obtain

$$\tilde{F}_\alpha(\mathbf{k},\omega)=4\pi B\sum_{l>0}F_{\alpha l}\sin(k_yy_j)\frac{\delta(\omega+v_dk_x)}{k_x+i\epsilon},\qquad(4)$$

where the index l refers to the lth lattice plane above and parallel with the cut plane with $\mathbf{F}_l$ being the Kanzaki force acting on every atomic row in this plane, and where $\epsilon\to0^+$ as implied by the Sokhotski-Plemelj formula [48]. The domain on which Eq. (4) is uniquely defined is $k_x\in[-\infty,\infty]$, $k_y\in[-k_y^b,k_y^b]$, where k_y^b is the maximum value of k_y found in the lattice Brillouin zone. This is because the Kanzaki force as defined in Eq. (3) breaks the crystal symmetry in the x direction only, leaving the y-direction translation symmetry intact. We can now evaluate the relative displacement between the rows immediately above and below the glide plane $\Delta u(x_i,t)=u_z(x_i,y_1,t)-u_z(x_i,y_{-1},t)$ as the screw dislocation passes. Combining Eqs. (2) and (4) this yields

$$\Delta u(x_i,t) = -\frac{4B}{k_y^b \pi M} \sum_{l>0,b,\beta} \int_0^{k_y^b} dk_y \int_0^{\infty} dk_x F_{\beta l} \sin(k_y y_j) \sin(k_y y_1) \tilde{u}_z(\mathbf{k},b) \tilde{u}_\beta^*(\mathbf{k},b) \times \left(\frac{(\omega^2(\mathbf{k},b) - v_d^2 k_x^2) \sin[k_x(x_i - v_d t)] + 2\Gamma v_d k_x \cos[k_x(x_i - v_d t)]}{(k_x + i\epsilon)[(\omega^2(\mathbf{k},b) - v_d^2 k_x^2)^2 + 4\Gamma^2 v_d^2 k_x^2]} - \frac{\pi \delta(k_x)}{2\omega^2(\mathbf{k},b)} \right). \quad (5)$$

Note that the last term of the integrand of Eq. (5) is ill defined as $\mathbf{k} \to (0,0)$. However, this singularity can be avoided using a $k_x = 1/\lambda$ substitution. All results were evaluated with the minimal Γ that ensured convergence of the results.

An in house code was written to evaluate Eq. (5), using cubature [49] for the numerical integration part. First, results were obtained for a square lattice with lattice constant a, and the dislocation line parallel to a cube edge. Atomic rows interact only with their nearest neighbors

$$U^h(u_{z,ij}) = \frac{K}{2} u_{z,ij}^2, \quad (6)$$

where K is the harmonic force constant and $u_{z,ij} = u_z(\mathbf{r}_i) - u_z(\mathbf{r}_j)$. This is the lattice as studied by Caro and Glass in Ref. [26] and drawn schematically in the inset of Fig. 1. In Fig. 1 we make three observations. First, a resonance is present for dislocations traveling at $v_d = 0.3c_t$, far below the shear wave speed of the lattice c_t. This is in agreement with previous studies on the mobility of a screw dislocation in comparable lattices [23–26]. These works also explain in detail why the resonance occurs at this velocity. The focus here is on the physical consequences of this resonance. With increasing velocity, we observe the expected screw dislocation behavior: as the dislocation passes x_i, $\Delta u(x_i)$ jumps from 0 to B, around which it oscillates with decreasing amplitude. The initial overshoot increases with increasing v_d and plateaus at $1.4B$. Finally, contrary to continuum model predictions [4,5] nothing extraordinary is seen to occur for $v_d = c_t$.

Equivalent results were obtained for a uniformly moving screw dislocation in bcc tungsten modeled using an embedded atom potential [50]. This provides a more realistic dispersion relation $\omega(\mathbf{k},b)$ compared to earlier lattice dynamics models [23–26]. Similar observations to those for the simple cubic lattice model manifested themselves in this case. A resonance was observed to occur around $v_d = 0.24c_t$. At higher speeds, the initial overshoot grew and peaked at $1.46B$ for $v_d = 0.97c_t$.

The simple cubic lattice dynamics model was compared with a MD simulation in an identical arrangement, where atomic rows interacted through a quartic interaction potential

$$U^q(u_{z,ij}) = \frac{Ka^2}{2} \left[\left(\frac{u_{z,ij}}{a} \mod 1 \right)^2 - 2 \left(\frac{u_{z,ij}}{a} \mod 1 \right)^4 \right] \quad (7)$$

such that $U^q(x) = U^q(x + na)$ for $n \in \mathbb{Z}$. A simple cubic lattice was constructed comprising 100 by 100 atoms along x and y axes, and just 1 atom along z with periodic boundary conditions in this direction. Free boundary conditions were used in the other two directions. A homogeneous shear stress $\sigma_{yz} = 13\sigma_{th}/20$ was applied to the lattice, where $\sigma_{th} = Ka/(3\sqrt{3})$ is the theoretical shear strength, and the lattice was relaxed. Then a screw dislocation was injected by instantaneously displacing the lattice planes $y = 50a$ and $y = 51a$ by $\pm a/2\hat{\mathbf{z}}$, respectively, for $x < 50a$. Subsequently, the MD simulation was run in the NVE ensemble while maintaining the uniform driving stress σ_{yz} and was stopped before the fastest traveling lattice waves emanating from the dislocation reached the box boundary. The dislocations were observed to reach their terminal velocity in only a few time units ($\sqrt{M/K}$) after their injection, in agreement with Ref. [29].

Figure 2 shows the observed $\Delta u(t)$ along the glide plane for $v_d = 0.72c_t$. It can be seen that at early times [$t < 35$ in Fig. 2(a)] the glide plane profile is exactly what one would expect for a propagating dislocation: $\Delta u = 0$ before and $\Delta u \approx B$ behind the dislocation. However, over time the initial overshoot increases in magnitude which builds up to

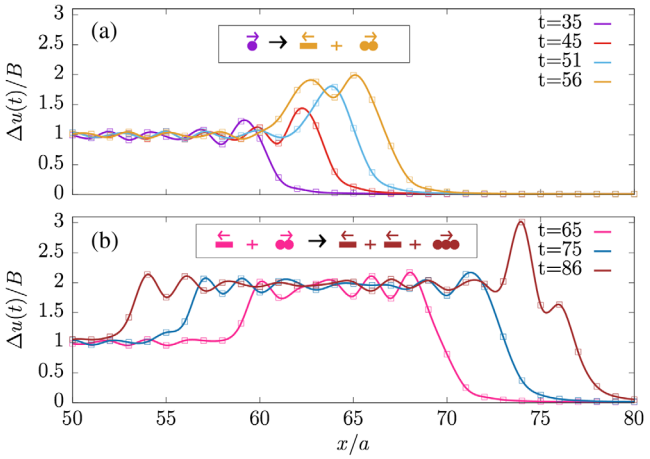

FIG. 2. $\Delta u(t)$ on the glide plane as observed in the MD with quartic interaction potential U^q at different times expressed in units of $\sqrt{M/K}$. A single dislocation is injected at $x = 50a$ at $t = 0$ and travels to the right. The first kinematic generation event is shown in (a), followed by the second event in (b). Their associated dislocation reactions are shown in the top insets where circles and rectangles represent screw dislocations of opposite handedness and the arrows above them indicate their directions of travel.

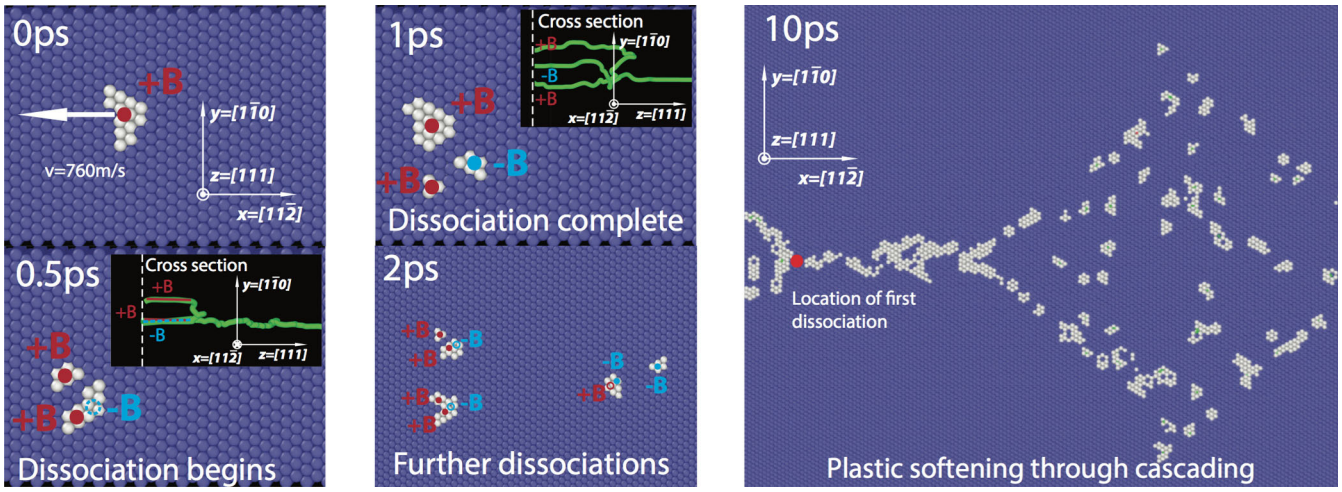

FIG. 3. Snaphsot of the kinematic generation dissociation process observable in MD simulations of bcc W at 125 K. The dislocation positions were found using the DXA algorithm [56] as implemented in Ovito [57]. White shaded particles indicate regions of considerable disregistry.

a critical point at which the dislocation causes a relative displacement jump of $2B$. This necessarily gives rise to a displacement jump of $-B$ behind the initial dislocation which can be seen to propagate in the opposite direction to the original dislocation. This is a kinematic generation mechanism [1] with dislocation reaction equation $B \Rightarrow 2B + -B$, represented in the top inset of Fig. 2. Following this initial generation event, the dislocations propagate until the same mechanism produces another kinematic generation event, shown in Fig. 2(b). It is clear that these are only the first two kinematic generation events of a subsequent cascade.

From the lattice dynamics model above we can explain this kinematic generation mechanism as follows: At resonant dislocation velocities, Δu exceeds $1.5B$ which will result in the kinematic generation mechanism discussed above. In the MD this critical point is reached more easily compared to the lattice dynamics model as the stiffness decreases with increasing separation between atoms. This shows that the lattice models can be considered to be a limiting case: if the overshoot goes beyond $1.5B$ in the lattice model, it is likely that this mechanism is accessible in a real crystal.

We have compared the tungsten lattice dynamics model to an equivalent MD simulation of a uniformly moving screw dislocation, employing LAMMPS [51,52] and an embedded atom interatomic potential developed for bcc W [50]. A $1/2\langle 111\rangle$ screw dislocation gliding along $x = [11\bar{2}]$ was initially inserted by displacing the perfect lattice atoms according to the displacement field predicted by elasticity using ATOMSK [53], in a box of dimensions $80\times50\times30$ unit cells with $x = [11\bar{2}]$, $y = [1\bar{1}0]$, $z = [111]$ subject to periodic boundary conditions. The system was then equilibrated using a conjugate gradient minimization to recover the 0 K dislocation structure [51,54], and then thermalized in the NVT ensemble for 10 ps to the target temperature. Subsequently, the MD simulation was run in the NVE ensemble by applying a constant force in the z direction on the first two top and bottom atomic layers (cf. Refs. [31,55]). To prevent overheating due to the applied loads, the second and third layers were thermalized in the NVT ensemble throughout (cf. Ref. [54]). As can be seen in the series of snapshots in Fig. 3, upon reaching a velocity of 709.74 ± 356.84 m/s at an external load of around 250 MPa, the original dislocation was seen to dissociate into a $+2B$ and a $-1B$ dislocation on different $\{112\}$ planes. This kinematic generation mechanism was observed for target temperatures of 10 K, 50 K, 125 K, 298 K, and 450 K and was solely dependent on the dislocation reaching the target critical velocity of $\approx 0.27c_t$. It is clear that this velocity has to be sustained for a couple of ps to give the generation mechanism time to act. This is in good agreement with the $v_d = 0.24c_t$ resonance determined from the tungsten lattice dynamics model. Further dissociations resulted in a cascade and substantial plastic softening of the system as shown in Fig. 3. The cascade is accompanied by dissipation of energy from the dislocation cores as heat. Thus, kinematic generation offers a feasible onset mechanism for adiabatic shear banding in loading regimes where dislocation speeds are large [38].

These MD simulations confirm the resonances determined in lattice dynamics models have physical significance: They introduce mechanical instabilities which activate kinematic generation of dislocations. This offers an alternative to previous interpretations in which the resonances were seen as insurmountable barriers to dislocation motion and dismissed as unphysical artifacts of lattice dynamics models [1]. This multiplication mechanism may explain previous observations of dislocation avalanches in MD simulations of edge dislocations [35,36]. This questions the continuum elasticity

view of kinematic generation as a core dissociation affecting only edge dislocations gliding above the Rayleigh wave speed [1,37,58].

The lattice resonances are purely a consequence of the radiation that emerges due to the periodic breaking and making of bonds across the cut plane as the dislocation moves through the crystal. This is why the instabilities are absent in continuum models. Furthermore, the quantitative agreement between the lattice dynamics models and their equivalent MD simulations in determining the resonant dislocation velocity suggests that the detail of the dislocation core structure is of secondary importance since the former do not include a core description and the latter do.

To accelerate dislocations beyond the speed of sound, it is likely they will have to pass through instabilities. These affect the motion of the dislocation qualitatively in one of two ways depending on the duration of the kinematic generation mechanism. If the dislocation is accelerated beyond the resonant velocity region quicker than the kinematic generation mechanism needs to act, the instability will be avoided. On the other hand, if the dislocation's acceleration is too small it may get trapped: At resonance the kinetic energy of atoms in the dislocation core will rise and be converted into the generation of dislocation pairs. The repetition of this process will prevent the dislocation from accelerating through the resonance. Thus, kinematic generation of dislocations is an avoidable barrier to supersonic dislocation motion, which depends on the time available for the mechanism to act. For example, injecting dislocations [28] at supersonic speeds avoids kinematic generation completely. However, it does render dislocation motion beyond them highly dependent on how the instabilities were surpassed. This may explain why despite the numerous MD simulations available in the literature [30–33,55,59] there is still no generally accepted dislocation mobility law at high dislocation speeds.

Whether there is sufficient time for a dislocation avalanche to develop will become an additional consideration in larger scale dislocation dynamics simulations [60–62] and in producing continuum plastic flow rules [63–65]. The velocities at which we observe kinematic generation are much lower than previously thought which will have implications for deformation processes at moderate strain rates, such as adiabatic shear banding [66], dynamic fracture [67,68], and in describing the Hugoniot state under ramp and shock loading [3]. This extends the relevance of kinematic generation to many industrially relevant processes such as machining [69], forging [70], and wear [71].

J. V. was supported through a studentship in the Centre for Doctoral Training on Theory and Simulation of Materials at Imperial College London funded by EPSRC under Grant No. EP/L015579/1. B. G.-L. is thankful to the Master and Fellows of Trinity College Cambridge for the financial support of the author as a Title A Fellow of Trinity College. D. D. also acknowledges the support of the EPSRC via his Established Career Fellowship EP/N025954/1.

*jv610@imperial.ac.uk
†bg374@cam.ac.uk

[1] J. P. Hirth and J. Lothe, *Theory of Dislocations*, reprint of 2nd ed. (Krieger Publishing Company, Malabar, 1992).
[2] F. A. Bandak, R. W. Armstrong, and A. S. Douglas, Phys. Rev. B **46**, 3228 (1992).
[3] M. A. Meyers, *Dynamic Behavior of Materials* (John Wiley, Hoboken, 1994).
[4] F. C. Frank, Proc. Phys. Soc. London Sect. A **62**, 131 (1949).
[5] J. D. Eshelby, Proc. Phys. Soc. London Sect. A **62**, 307 (1949).
[6] J. D. Eshelby, Phys. Rev. **90**, 248 (1953).
[7] W. G. Johnston and J. J. Gilman, J. Appl. Phys. **30**, 129 (1959).
[8] J. Gorman, D. Wood, and T. Vreeland Jr., J. Appl. Phys. **40**, 833 (1969).
[9] A. P. L. Turner and T. Vreeland Jr., Acta Metall. **18**, 1225 (1970).
[10] W. D. Nix and R. A. Menezes, Annu. Rev. Mater. Sci. **1**, 313 (1971).
[11] J. D. Eshelby, Proc. Phys. Soc. London **69**, 1013 (1956).
[12] J. Weertman, in *Response of Metals to High Velocity Deformation*, edited by P. G. Shewmon and V. F. Zackay, Metallurgical Society Conferences, Metallurgical Society of AIME, Vol. 9 (Interscience, New York, 1961), pp. 205–249.
[13] P. P. Gillis and J. Kratochvil, Philos. Mag. **21**, 425 (1970).
[14] J. Weertman, J. Appl. Phys. **38**, 5293 (1967).
[15] X. Markenscoff, J. Elast. **10**, 193 (1980).
[16] X. Markenscoff and R. J. Clifton, J. Mech. Phys. Solids **29**, 253 (1981).
[17] J. P. Hirth, H. M. Zbib, and J. Lothe, Model. Simul. Mater. Sci. Eng. **6**, 165 (1998).
[18] Y.-P. Pellegrini, Phys. Rev. B **90**, 054120 (2014).
[19] X. Markenscoff and L. Ni, J. Mech. Phys. Solids **49**, 1603 (2001).
[20] I. A. Kunin, in *Mechanics of Generalized Continua* (Springer, New York, 1968), pp. 321–329.
[21] M. Lazar and Y.-P. Pellegrini, J. Mech. Phys. Solids **96**, 632 (2016).
[22] J. D. Clayton and J. T. Lloyd, J. Phys. Commun. **2**, 045032 (2018).
[23] W. Atkinson and N. Cabrera, Phys. Rev. **138**, A763 (1965).
[24] V. Celli and N. Flytzanis, J. Appl. Phys. **41**, 4443 (1970).
[25] S. Ishioka, J. Phys. Soc. Jpn. **30**, 323 (1971).
[26] J. A. Caro and N. Glass, J. Phys. (Paris), Lett. **45**, 1337 (1984).
[27] B. Gurrutxaga-Lerma, Model. Simul. Mater. Sci. Eng. **24**, 065006 (2016).
[28] P. Gumbsch and H. Gao, Science **283**, 965 (1999).
[29] H. Koizumi, H. O. K. Kirchner, and T. Suzuki, Phys. Rev. B **65**, 214104 (2002).

[30] Z. Jin, H. Gao, and P. Gumbsch, Phys. Rev. B **77**, 094303 (2008).
[31] H. Tsuzuki, P. S. Branicio, and J. P. Rino, Appl. Phys. Lett. **92**, 191909 (2008).
[32] H. Tsuzuki, P. S. Branicio, and J. P. Rino, Acta Mater. **57**, 1843 (2009).
[33] C. J. Ruestes, E. M. Bringa, R. E. Rudd, B. A. Remington, T. P. Remington, and M. A. Meyers, Sci. Rep. **5**, 16892 (2015).
[34] J. Marian and A. Caro, Phys. Rev. B **74**, 024113 (2006).
[35] J. H. Weiner and M. Pear, Philos. Mag. **31**, 679 (1975).
[36] J. Schiøtz, K. W. Jacobsen, and O. H. Nielsen, Philos. Mag. Lett. **72**, 245 (1995).
[37] Lomdahl and Srolovitz, Phys. Rev. Lett. **57**, 2702 (1986).
[38] R. W. Armstrong and W. L. Elban, Mater. Sci. Eng. A **122**, L1 (1989).
[39] H. Kanzaki, J. Phys. Chem. Solids **2**, 24 (1957).
[40] N. W. Ashcroft and N. D. Mermin, *Solid State Physics* (Brooks/Cole, Belmont, 1976).
[41] A. A. Maradudin, J. Phys. Chem. Solids **9**, 1 (1959).
[42] N. E. Glass, J. Phys. (Paris), Lett. **44**, 741 (1983).
[43] B. Gurrutxaga-Lerma and J. Verschueren (unpublished).
[44] Roman indices run over all particles in a lattice, Greek indices run over Cartesian axes.
[45] A. A. Maradudin, Rep. Prog. Phys. **28**, 331 (1965).
[46] E. N. Economou, *Green's Functions in Quantum Physics*, 3rd ed. (Springer, Berlin, 2006).
[47] L. L. Boyer and J. R. Hardy, Philos. Mag. **24**, 647 (1971).
[48] A. I. Markushevich, *Theory of Functions of a Complex Variable* (American Mathematical Society, Providence, 2005), Vol. I.
[49] https://github.com/stevengj/cubature.
[50] M.-C. Marinica, L. Ventelon, M. R. Gilbert, L. Proville, S. L. Dudarev, J. Marian, G. Bencteux, and F. Willaime, J. Phys. Condens. Matter **25**, 395502 (2013).
[51] S. Plimpton, J. Comp. Physiol. **117**, 1 (1995).
[52] http://lammps.sandia.gov.
[53] P. Hirel, Comput. Phys. Commun. **197**, 212 (2015).
[54] M. R. Gilbert, S. Queyreau, and J. Marian, Phys. Rev. B **84**, 174103 (2011).
[55] D. L. Olmsted, L. G. HectorJr, W. A. Curtin, and R. J. Clifton, Model. Simul. Mater. Sci. Eng. **13**, 371 (2005).
[56] A. Stukowski, V. V. Bulatov, and A. Arsenlis, Model. Simul. Mater. Sci. Eng. **20**, 085007 (2012).
[57] A. Stukowski, Model. Simul. Mater. Sci. Eng. **18**, 015012 (2010).
[58] J. Weertman and J. Weertman, *Dislocations in Solids*, edited by F. R. N. Nabarro, Moving Dislocations, Vol. 3 (North-Holland Publishing Company, Amsterdam, Oxford, 1980).
[59] J. Cho, J.-F. Molinari, and G. Anciaux, Int. J. Plast. **90**, 66 (2017).
[60] B. Gurrutxaga-Lerma, D. S. Balint, D. Dini, D. E. Eakins, and A. P. Sutton, Phys. Rev. Lett. **114**, 174301 (2015).
[61] M. A. Shehadeh, E. M. Bringa, H. M. Zbib, J. M. McNaney, and B. A. Remington, Appl. Phys. Lett. **89**, 171918 (2006).
[62] V. V. Bulatov and W. Cai, *Computer Simulations of Dislocations* (Oxford University Press, Oxford, 2006).
[63] E. Orowan, Proc. Phys. Soc. London **52**, 8 (1940).
[64] R. A. Austin and D. L. McDowell, Int. J. Plast. **27**, 1 (2011).
[65] Z. Zhang, D. E. Eakins, and F. P. Dunne, Int. J. Plast. **79**, 196 (2016).
[66] B. Dodd and Y. Bai, *Adiabatic Shear Localization: Frontiers and Advances* (Elsevier, New York, 2012).
[67] L. B. Freund, *Dynamic Fracture Mechanics*, Cambridge Monographs on Mechanics (Cambridge University Press, Cambridge, England, 1990).
[68] V. Rajan and W. Curtin, J. Mech. Phys. Solids **90**, 18 (2016).
[69] T. Childs, K. Maekawa, T. Obikawa, and Y. Yamane, *Metal Machining: Theory and Applications* (Arnold, London, 2000).
[70] W. Hosford and R. Caddell, *Metal Forming: Mechanics and Metallurgy* (Cambridge University Press, Cambridge, England, 2011).
[71] R. Aghababaei, T. Brink, and J.-F. Molinari, Phys. Rev. Lett. **120**, 186105 (2018).